

Autowave Plasticity: Principles and Possibilities

L. B. Zuev^{a,*} and S. A. Barannikova^a

^a*Institute of Strength Physics and Materials Science, Siberian Branch, Russian Academy of Sciences, Tomsk, 634055 Russia*

**e-mail: lbz@ispms.tsc.ru*

Received February 15, 2019; revised February 15, 2019; accepted November 21, 2019

Abstract—Basic concepts of the autowave model of development of a localized plastic flow of solids of different natures are considered. It is shown that plastic deformation develops in a localized (at the macroscale level) way throughout the process. The form of the observed localization patterns is related to stages of strain hardening of the material. The patterns are projections of different modes of the localized plastic flow autowave on the observation surface. An elastoplastic strain invariant is introduced, which is considered as the main equation of the autowave plasticity model, and its physical nature is discussed.

DOI: 10.1134/S1063784220050266

INTRODUCTION

The physical nature of plastic deformation of solids has not been comprehensively studied; the solution of this problem is hindered by difficulties related to the consideration of nonlinearity and activity of the deformed medium [1]. Nevertheless, certain progress in plasticity physics has occurred in recent years; this progress was entailed by the detection and confirmation of the macroscale spatial–temporal character of the solid plastic flow in all stages of the forming process [2, 3]. These concepts originate from the study by Seeger and Frank [4], where the development of localized plastic deformation was interpreted as self-organization of the deformed medium; thus, the problem of plasticity physics was brought into the range of interests of synergetics. The definition of self-organization proposed by Haken [5] (“A system is referred to as self-organizing if it acquires some spatial, time, or functional structure without a specific external effect”) was found convenient to be used in plasticity physics. Finally, Nicolis and Prigogine [6] directly noted that “the nature of plastic flow should be discussed within the theory of nonlinear dynamic systems.”

To date, in the physics of plasticity, two aspects of research are relevant, differing in the scale of the studied objects, but operating with the concept of structure formation. The first one is related to analysis of formation of dislocation substructures during plastic flow in a small volume of the material [7]. It requires spatial resolution at the level of individual dislocations with their characteristic Burgers vector scale $b \approx 10^{-10}$ m. The second aspect originating from [4–6] concerns investigation of macroscopic ($L \approx 10^{-3}$ – 10^{-2} m) regularities of localization of plastic flow in the entire sam-

ple volume. We developed this line of research in, e.g., [2, 3]. Phenomena studied within these approaches differ significantly in their scales ($L/b \approx 10^7$ – 10^8).

Now it is clear that all stages of the deformation process are characterized by macroscopic localization of plastic flow [2]. It manifests itself in spontaneous stratification of the deformed material into correlated deforming and nondeforming (at a given instant) volumes. The presence of this correlation makes it possible to consider plastic flow as self-organization of the deformed medium taking various forms.

In this study, we discuss the experimentally revealed macroscopic regularities of spontaneous nucleation and evolution of the strain localization at different stages of the deformation process in tension with a constant rate (active loading) and make an attempt to establish a direct relationship between the lattice characteristics and the regularities of localized plastic flow and to explain the nature of this relationship.

1. PATTERNS AND AUTOWAVES OF LOCALIZED PLASTIC FLOW

1.1. Strain Localization. Patterns

The macroscopic spatial distributions of the localized strain (localization patterns), which are observed during plastic flow and evolving in time, are spontaneously generated during tension of samples with a constant rate [2]. In the general sense, the popular term “pattern” means “any sequence of phenomena in time or any position of objects in space, which can be distinguished from other sequences or other positions or compared with them” [8]. In the case of plastic strain, the localized plasticity pattern is a consistently

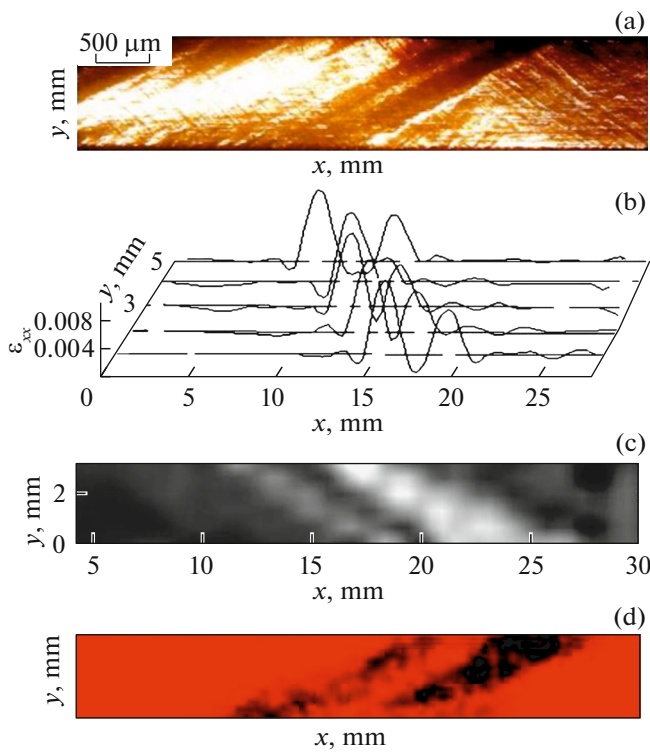


Fig. 1. Pattern of localized plasticity at deformation of a Fe–3 wt % Si single crystal: (a) micrograph, (b) distribution of the plastic distortion tensor component, (c) half-tone image, and (d) digital speckle photography image.

evolving set of macroscopic zones of localized plasticity. Plastic flow localization patterns were experimentally found by us using speckle photography [2, 3]; their existence was later confirmed by other researchers using the methods of digital image correlation [9–11] and IR imaging [12]. A typical example of a localization pattern is shown in Fig. 1.

Systematization of the observations results showed that, at plastic flow, the pattern configurations are related to the stages of strain hardening, which can be distinguished when analyzing the stress–strain curves of plastic flow $\sigma(\epsilon)$. At least, the number of pattern configurations coincides with the number of stages of the plastic flow curve of a given material.

This regularity was noted for all investigated materials, irrespective of their composition, structure, and plastic deformation mechanism [2]. Even rather large variations in these characteristics induce only small quantitative changes in localization patterns, barely changing their forms. The localized plasticity patterns are observed on free surfaces of strained samples; however, the corresponding deformation phenomena occur throughout the entire volume of the deformed material.

1.2. Autowave Modes of Localized Plastic Flow

A hypothesis was suggested [13] based on the analysis of a set of pattern forms, according to which the development of localized plastic deformation is an autowave process [14]. Such processes describe mechanisms of structure formation in active media (i.e., media containing distributed energy sources in their volume). The deformed medium can be considered as active, because it contains volume-distributed concentrators of elastic stress serving as these sources. In essence, the patterns are observed projections of autowave modes of localized plastic flow arising in the volume of the deformed medium to the sample surface. This suggestion is based on the analysis of their forms and kinetics in different stages of deformation and confirmed by observations of pattern evolution in many deformed materials. The experimental technique used for observing the patterns yielded quantitative characteristics of the localized plasticity autowaves. These characteristics generally include spatial ($\lambda = 2\pi/k$) and temporal ($T = 2\pi/\omega$) process periods and velocity of plastic deformation zones $V_{aw} = \lambda/T = \omega/k$. Here, k and ω are the wave number and frequency, respectively. The values of λ and T are measured using the “deformation zone position X –time t ” (X – t) diagrams [2], an example of which is shown in Fig. 2. The possibility of obtaining information about parameters k , L. B. Zuev and S. A. Barannikova, and V_{aw} makes it possible to bring the discussion of plastic flow localization phenomenon to the quantitative level.

Hence, to gain insight into the nature of autowave deformation, we consider the spatial–temporal transformation of stress field $\sigma(x, y, t)$ and plastic strain field $\epsilon(x, y, t)$. It is based on interrelated elastic and plastic displacements of particles of the medium u ; notably, the stress transformation causes strain, whereas a change in the strain induces transformation of the stress field. The process rates are limited by elastic-wave velocity V_l for the elastic field and localization autowave velocity V_{aw} for the plastic strain field.

At a small deviation of the deformed system from equilibrium, primary (p) displacement velocities $\dot{u}^{(p)}$ are proportional to the gradients of plastic and elastic strains, i.e., $\dot{u}_{pl}^{(p)} \approx D_{\epsilon\epsilon} \nabla \epsilon_{pl}$ and $\dot{u}_{el}^{(p)} \approx D_{\sigma\sigma} \nabla \epsilon_{el}$. The cross effects must also be taken into account by introducing additional (ad) velocities $\dot{u}_{el}^{(ad)} \approx D_{\epsilon\sigma} \nabla \epsilon_{pl}$ and $\dot{u}_{pl}^{(ad)} \approx D_{\sigma\epsilon} \nabla \epsilon_{el}$. Now, we find for total velocities $\dot{u}_{pl} = \dot{u}_{pl}^{(p)} + \dot{u}_{pl}^{(ad)}$ and $\dot{u}_{el} = \dot{u}_{el}^{(p)} + \dot{u}_{el}^{(ad)}$ that

$$\begin{cases} \dot{u}_{pl} = D_{\epsilon\epsilon} \nabla \epsilon_{pl} + D_{\epsilon\sigma} \nabla \epsilon_{el}, & (1) \\ \dot{u}_{el} = D_{\sigma\epsilon} \nabla \epsilon_{el} + D_{\sigma\sigma} \nabla \epsilon_{pl}. & (2) \end{cases}$$

With allowance for the relationship between the elastic and plastic strains, the following matrix can be

formed using the coefficients of this system of equations [15]:

$$\mathbf{D} = \begin{bmatrix} D_{\varepsilon\varepsilon} & D_{\varepsilon\sigma} \\ D_{\sigma\varepsilon} & D_{\sigma\sigma} \end{bmatrix}, \quad (3)$$

the elements of this matrix obviously have a dimension of $\text{m}^2 \text{s}^{-1}$. Here, diagonal elements $D_{\varepsilon\varepsilon}$ and $D_{\sigma\sigma}$ characterize the main fluxes of displacement vectors, while off-diagonal elements $D_{\varepsilon\sigma}$ and $D_{\sigma\varepsilon}$ correspond to the cross effects.

Equations (1) and (2) are similar to the first Fick law for diffusion $\dot{u} \sim D\nabla\varepsilon$. Afterwards, after passage to the second Fick law in the form of $\dot{\varepsilon} \sim D\varepsilon''$, one should take into account that the Kolmogorov–Petrovskii–Piskunov equation [14, 16] $\dot{y} = \Phi(x) + Dx''$ is generally used to describe autowave processes, which is obtained by adding nonlinear function $\Phi(x)$ to the right-hand side of the second Fick equation.

The general description of autowave generation in active media is traditionally constructed based on the consideration of competition of antagonistic factors: activating (autocatalytic) and inhibiting (damping) [14]. During plastic flow, the process activator is plastic strain ε and the inhibitor is stress σ [2]. Therefore, in accordance with [16], the activator and inhibitor change rates can be written as, respectively,

$$\begin{cases} \dot{\varepsilon} = f(\varepsilon, \sigma) + D_{\varepsilon\varepsilon}\varepsilon'', & (4) \\ \dot{\sigma} = g(\varepsilon, \sigma) + D_{\sigma\sigma}\sigma''. & (5) \end{cases}$$

With allowance for the dimension and physical meaning, transport coefficients $D_{\varepsilon\varepsilon}$ and $D_{\sigma\sigma}$ in differential autowave equations (4) and (5) can be identified with the diagonal components of matrix (3). The right-hand sides of Eqs. (4) and (5) include the hydrodynamic and diffusion components. The former is presented in these equations by nonlinear N -shaped functions $f(\varepsilon, \sigma)$ and $g(\sigma, \varepsilon)$, describing the strain and stress change rates during a unit relaxation event, and is related to the displacement of the deformation front along the sample at relaxation of local stress concentrators. The latter component is determined by diffusion-like terms $D_{\varepsilon\varepsilon}\partial^2\varepsilon/\partial x^2$ and $D_{\sigma\sigma}\partial^2\sigma/\partial x^2$ and initiates the nucleation of the plastic deformation zone at macroscopic distance $\sim\lambda$ from the existing front due to relaxation of a concentrator in this region (the so-called throw of deformation).

1.3. The Nature of Plastic Flow Localization Autowaves

Autowaves in active nonlinear media form various modes the type of which is mainly determined by the actual strain hardening law. In almost all cases, the autowave is a set of local plastic flow zones developing in a correlated way, and its generation is caused by the throw effect. Indeed, according to the Taylor–Orowan equation $\dot{\varepsilon} \approx b\rho_{\text{md}}V_{\text{disl}}$ [17], the condition of constancy of strain rate $\dot{\varepsilon} = \text{const}$ set by a testing machine is sat-

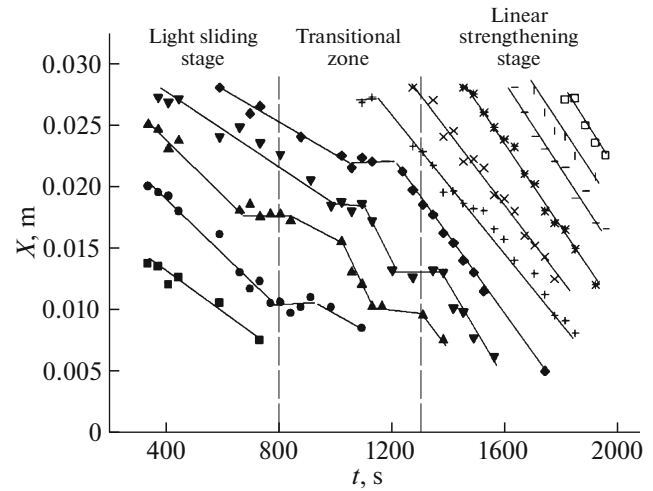


Fig. 2. X - t strain diagrams of single crystals of high-nitrogen manganese stainless steel with the extension axis oriented along the $[\bar{1}11]$ axis.

isfied at $\rho_{\text{md}}V_{\text{disl}} = \text{const}$, i.e., at sufficient mobile dislocation density ρ_{md} and dislocation velocity V_{disl} . If this requirement is violated because of a decrease in the density of mobile dislocations at strain hardening or the drop in their velocity with a decrease in the effective stress exerted on a dislocation from σ to $\sigma \sim Gb\sqrt{\rho_d}$ [17], the condition $\dot{\varepsilon} = \text{const}$ should be provided by an additional contribution from diffusion-like term $D_{\varepsilon\varepsilon}\varepsilon''$. This contribution arises during generation of a new localized strain zone at distance $\sim\lambda$ from the initial one (i.e., during formation of a localized plastic flow autowave).

2. ANALYSIS OF COEFFICIENT MATRIX (3)

2.1. Diagonal Elements

It can be suggested from physical considerations that coefficients $D_{\varepsilon\varepsilon}$ and $D_{\sigma\sigma}$ in Eqs. (4) and (5) are equivalent to diagonal elements of matrix (3). The former is related to density of mobile dislocations ρ_{md} , while the latter is determined by the stress field. Then, by analyzing dimensions, we obtain

$$D_{\varepsilon\varepsilon} \approx \frac{d(\rho_{\text{md}})^{-1}}{dt} \quad (6)$$

and

$$D_{\sigma\sigma} \approx \sqrt{\frac{F}{\rho_0}}, \quad (7)$$

where F is the sample tension force during the test and ρ_0 is the density of the medium. One might suggest that, by analogy with [14], the variety of autowave modes of the localized plastic flow and, accordingly, observed localized strain patterns depends on the ratio of coefficients $D_{\varepsilon\varepsilon}$ and $D_{\sigma\sigma}$ in Eqs. (4) and (5). There-

fore, possible versions of the ratio of these coefficients should first be qualitatively considered.

(i) $D_{\sigma\sigma} = 0$, $D_{\varepsilon\varepsilon} \neq 0$. Nullification of the second term in Eq. (5) reduces the role of the stress as a factor slowing down the development of plastic flow. This corresponds to the case of strain without hardening and, apparently, is consistent with the situation where a unit plastic flow front (Luders front) moves along the sample with a constant velocity [18]. The dynamics of events in this case is determined by relaxation events at the front of this band (in fact, by only the first terms on the right-hand sides of Eqs. (4) and (5)). In terms of the autowave process theory, this corresponds to a switching autowave in a bistable medium. At its front, the deformed material passes from the elastic to plastically deformed state at $\sigma = \text{const}$. The medium is bistable in this case [14] because the moving Luders front separates regions of the material with significantly different densities of mobile dislocations, separating, actually, two states with different strains.

(ii) $D_{\sigma\sigma} \approx D_{\varepsilon\varepsilon}$. Equality of transport coefficients corresponds to the case of synchronous propagation of plastic and elastic phenomena in the deformed medium, when the elastic and plastic strains follow each other. In this case, the phase of the arising autowave is constant, i.e., $\omega t - kx = \text{const}$. This situation is consistent with the existence of a phase autowave that is characteristic of easy glide and linear strain hardening stages when $\sigma \sin \varepsilon$. In these stages, as is shown in Fig. 2, one can observe movement of a group of equidistantly arranged localization zones along the sample with a constant velocity. It is known [14] that phase autowaves arise in systems consisting of self-oscillating elements during incomplete synchronization. A fundamental possibility of the existence of self-oscillating modes in dislocation ensembles was established in [19]. In these modes, the same volumes of the material can be multiply excited with a time interval determined by the microscopic properties of the medium. Phase autowaves have typical wave characteristics: wavelength, oscillation frequency, and propagation velocity.

(iii) $D_{\sigma\sigma} \gg D_{\varepsilon\varepsilon}$. At this ratio of the transport coefficients, the damping factor plays a key role in the formation of the deformation structure. Rapidly propagating elastic waves generate a standing elastic wave in the deformed sample, at the antinodes of which plastic strain is localized. This corresponds to the occurrence of a stationary dissipative structure in the stage of parabolic hardening when $\sigma \sin \sqrt{\varepsilon}$ [16], and a system of equidistant immobile zones of localized strain arises in the sample.

(iv) $D_{\sigma\sigma} \ll D_{\varepsilon\varepsilon}$. When passing to the final stage of the deformation process, the role of elastic stress becomes less important. This situation can be considered as generation of the "mode with sharpening" [20] leading to the formation of the only strain zone, i.e., to macroscopic localization of plastic flow and forma-

tion of the fracture neck. The mode of collapse of the localized plastic flow autowave [21] is implemented in this case; this collapse begins as a result of the matched movement of plasticity zones and ends with viscous fracture of the sample.

2.2. Correspondence Rule

Comparison of the data on the localization patterns with strain hardening stages showed that a specific pattern (projection of a certain autowave mode) is formed in each stage of plastic flow. This observation (valid for all materials investigated to date) suggested that there is a relationship, on the one hand, between the patterns and stages of strain hardening and, on the other hand, between the strain hardening stages and corresponding autowave modes.

According to the above-considered cases, one can state the following, in correspondence with the accepted terminology [14]:

(i) Stage of the yield plateau corresponds to the switching autowave.

(ii) Stage of linear strain hardening corresponds to the phase autowave.

(iii) Stage of parabolic strain hardening corresponds to the stationary dissipative structure.

(iv) Stage of prefracture corresponds to the autowave process collapse.

Therefore, the multistage process of plastic flow can be considered as a systematic change of autowave localization modes. This change is implemented in the following order: switching autowave \rightarrow phase autowave \rightarrow stationary dissipative structure \rightarrow autowave collapse.

An important feature of the localized plasticity autowave evolution in the deformed medium consists in the following. It is known [14] that experimental investigation of different autowave modes in chemical or biological systems requires designing specific generators for each process. The generators differ by type or kinetics of chemical reactions therein, chemical composition, temperature regime, sizes, and some other characteristics. In contrast, during deformation, autowave modes are generated under tension with a constant rate (i.e., with much less experimental difficulties). From this point of view, the deformed sample is a universal generator of autowave processes, which is convenient for both their simulation and experimental analysis [22].

2.3. Off-Diagonal Elements and Elastioplastic Invariant

Let us now consider off-diagonal elements $D_{\varepsilon\sigma}$ and $D_{\sigma\varepsilon}$ of transport-coefficient matrix (5), which are responsible for the cross-linking bond between stress and strain during plastic flow. In this case, according to the Onsager kinetic coefficient symmetry principle [15], these elements are equal, i.e., $D_{\varepsilon\sigma} \approx D_{\sigma\varepsilon}$. With

allowance for the dimension of elements, we can suggest that $\lambda V_{aw} \equiv D_{\varepsilon\sigma}$ and $\chi V_t \equiv D_{\sigma\varepsilon}$ and pass to equality $\lambda V_{aw} \approx \chi V_t$, where χ is the interplanar spacing and V_t is the propagation velocity of transverse ultrasonic oscillations. An experimental check of this suggestion yielded an important result. It was found that the following ratio is valid for different materials that exhibit a stage of linear strain hardening during plastic flow:

$$\frac{\lambda V_{aw}}{\chi V_t} \approx \frac{1}{2}. \quad (8)$$

Equation (8) referred to as the elastoplastic strain invariant [2] quantitatively relates the elastic-wave characteristics (χ and V_t) with the characteristics of plastic flow localization autowaves (λ and V_{aw}), combining the elastic ($\varepsilon_{el} \ll 1$) and plastic ($\varepsilon_{pl} \approx 1$) strains.

To specify the meaning of invariant (8), we take into account that χ and $\lambda \gg \chi$ in Eq. (8) are spatial scales of the elastic and plastic strain fields, while velocities V_t and $V_{aw} \ll V_t$ determine the kinetics of their transformation processes. In this case, Eq. (8) written in form

$$\frac{\lambda V_{aw}}{\chi V_t} = \frac{\lambda V_{aw}}{\chi V_t} = \frac{\lambda/\chi}{V_t/V_{aw}} = \hat{Z} \approx \frac{1}{2}, \quad (9)$$

reduces invariant (8) to the ratio of the scale ($\lambda/\chi \gg 1$) and kinetic ($V_t/V_{aw} \gg 1$) factors, which can now be considered as thermodynamic probabilities [15, 23]. The first one characterizes the number of possible zones of nucleation of the localized plastic strain autowave, while the second probability determines the choice of the autowave velocity from the range of its possible values ($0 \leq V_{aw} \leq V_t$) in the deformed system.

Then, Eq. (9) is related to changes in the entropy during the formation of localized plastic flow autowaves. In view of the additivity of the entropy, we write its total change as a sum of the scale and kinetic contributions:

$$\Delta S = \Delta S_{scale} + \Delta S_{kin} < 0. \quad (10)$$

Condition $\Delta S < 0$ indicates a decrease in the entropy during the formation of plastic flow localization autowaves [23]. To satisfy this condition, at least one term in Eq. (10) must be negative.

Using the Boltzmann formula, we write the scale contribution to the entropy as

$$\Delta S_{scale} = k_B \ln \frac{\lambda}{\chi} > 0, \quad (11)$$

where k_B is the Boltzmann constant. On the assumption (as was noted above) that the kinetic contribution to entropy is negative, we have

$$\Delta S_{kin} = -k_B \ln \frac{V_t}{V_{aw}} = k_B \ln \frac{V_{aw}}{V_t} < 0. \quad (12)$$

The opposite signs of parameters $\Delta S_{scale} > 0$ and $\Delta S_{kin} < 0$ in Eqs. (11) and (12) indicate the difference

in the contributions from the scale and kinetic factors to the character of development of the localized plastic deformation and directly to the formation of localized plastic flow autowaves. It follows from Eqs. (10)–(12) that

$$\ln \frac{\lambda}{\chi} - \ln \frac{V_t}{V_{aw}} = \Delta S/k_B < 0 \quad (13)$$

and, accordingly,

$$\hat{Z} = \frac{\lambda V_{aw}}{\chi V_t} = \frac{\lambda/\chi}{V_t/V_{aw}} = \exp(\Delta S/k_B). \quad (14)$$

Finally, we have

$$\hat{Z} \approx 1/2 \approx \exp(\Delta S/k_B). \quad (15)$$

In this case, the total decrease in entropy during the formation of a localized plasticity autowave is $\Delta S = k_B \ln(1/2) \approx -0.7k_B$.

Note that elastoplastic strain invariant (8) is the main equation of the developed autowave mechanics of plasticity [2, 3]. It entails a number of consequences [24] describing the main regularities of development of the localized plastic flow.

3. STATISTICAL ANALYSIS OF THE VALUES OF THE STRAIN INVARIANT

The evident importance of invariant relation (8) stimulates considerations of its generality and character of distribution of its experimental values. Hence, the focus of this study is on the need to investigate as many plastic materials as possible in order to ensure the universality of the data. These materials and the characteristics of autowave processes obtained for them are listed in Tables 1–3; it can be seen that the invariant was determined for the following cases:

- (i) Linear strain hardening and easy glide in metals [2].
- (ii) Phase transformation strain in intermetallic compound NiTi [25].
- (iii) Compressive strain in alkali halide crystals (KCl, NaCl, and LiF) [26].
- (iv) Compressive strain in rocks [27].
- (v) Creep in polycrystalline aluminum [28].
- (vi) Deformations due to the motion of individual dislocations in Zn, CsI, NaCl, KCl, and LiF single crystals [29–32] (in this case, the mean free path of dislocations was used instead of the localized strain autowave length).

Thus, single-crystal and polycrystalline materials deforming by slip, twinning (γ -Fe, marble), phase transformation (NiTi), and grain-boundary processes (sandstone) were considered. The stress–strain curves $\sigma(\varepsilon)$ of all the investigated materials include portions, in which phase localized plastic flow autowave were recorded.

Table 1. Comparison of the χV_t and λV_{aw} values for metals

$10^7 \text{ m}^2/\text{s}$	Stage of linear strain hardening												
	Cu	Zn	Al	Zr	Ti	V	Nb	α -Fe	γ -Fe	Ni	Co	Mo	
λV_{aw}	3.6	3.7	7.9	3.7	2.5	2.8	1.8	2.55	2.2	2.1	3.0	1.2	
χV_t	4.8	11.9	7.5	11.9	7.9	6.2	5.3	4.7	6.5	6.0	6.0	7.4	
$\lambda V_{aw}/\chi V_t$	0.75	0.3	1.1	0.3	0.3	0.45	0.33	0.54	0.34	0.35	0.5	0.2	
$10^7 \text{ m}^2/\text{s}$	Stage of linear strain hardening							Stage of easy glide					
	Sn	Mg	Cd	In	Pb	Ta	Hf	α -Fe	γ -Fe	Cu	Zn	Ni	Sn
λV_{aw}	2.4	9.9	0.9	2.6	3.2	1.1	1.0	7.4	2.9	1.9	1.0	1.3	3.3
χV_t	5.3	15.8	3.5	2.2	2.0	4.7	4.2	6.5	6.0	4.7	5.0	6.0	4.9
$\lambda V_{aw}/\chi V_t$	0.65	0.63	0.2	1.2	1.6	0.2	0.24	1.1	0.49	0.4	0.2	0.2	0.67

For 38 investigated materials, particular values of the $\lambda V_{aw}/\chi V_t$ ratio were established, its mean value $\langle \lambda V_{aw}/\chi V_t \rangle$ and dispersion σ^2 were found, and the mean square error of the mean result $\pm \sqrt{\sigma^2/n}$ was calculated [33]. As a result of these procedures, it was found that

$$\left\langle \frac{\lambda V_{aw}}{\chi V_t} \right\rangle = \left\langle \frac{\lambda \chi}{V_t/V_{aw}} \right\rangle = \langle \hat{Z} \rangle_{n=38} = 0.48 \pm 0.04. \quad (16)$$

The distribution law of the experimental sample of \hat{Z} values is important for understanding the nature of invariant relation (8). As a hypothesis, it is assumed that the \hat{Z} values are distributed according to the normal law, i.e., they do not correlate to any material characteristic. To check the hypothesis, variational series $\hat{Z}_1 < \hat{Z}_2 < \hat{Z}_3 < \dots < \hat{Z}_i < \dots < \hat{Z}_{n-1} < \hat{Z}_{n=38}$ was constructed using the data from Tables 1–3 [33]. Its terms are arguments for searching for numerical values of the normal distribution quantiles $-\infty < Q < \infty$ corresponding to $i/(n+1)$ values. The distribution is considered as normal if Q is linear with respect to \hat{Z} .

As can be seen in Fig. 3a, the linear character of dependence $Q(\hat{Z})$ is violated for indium and lead ($\hat{Z}_{In} = 0.96$ and $\hat{Z}_{Pb} = 1.3$). To estimate the possibility of assigning these values to gross errors and exclude them from further calculations, we applied statistical analysis using the criteria of [33] and

$$v_n = \frac{|\langle \hat{Z} \rangle - \hat{Z}_{In}|}{\sqrt{\sigma^2}} = 1.92$$

$$\text{and } v_n = \frac{|\langle \hat{Z} \rangle - \hat{Z}_{Pb}|}{\sqrt{\sigma^2}} = 3.28, \quad (17)$$

where $\hat{Z}_{In} = 0.96$ and $\hat{Z}_{Pb} = 1.3$ are the maximum values for the sample under study. The possibility of excluding these data from analysis is confirmed by nonfulfilment of the inequality $v_n < v_{max}$. It follows from the reference tables [33] that $v_n > v_{max} = 3.259$ for lead, so that the value $\hat{Z}_{Pb} = 1.3$ can be excluded from the sample as is shown in Fig. 3b.

After excluding the gross error of $\hat{Z}_{Pb} = 1.3$, the new mean invariant value is $\langle \hat{Z} \rangle_{n=37} = 0.45 \pm 0.04$ at the correlation coefficient between parameters Q and \hat{Z} of $\sim 0.98 \approx 1$. Apparently, with allowance for the accuracy attained in the experiments, it should be assumed that $\langle \hat{Z} \rangle_{n=38} \approx \langle \hat{Z} \rangle_{n=37} \approx \langle \hat{Z} \rangle \approx \frac{1}{2}$. An analysis confirmed that changes in the elastoplastic invariant value in the range of $0.2 \leq \hat{Z} \leq 1.3$ are related only to the experimental errors in measuring λ and V_{aw} . This means that the elastoplastic strain invariant can be applied for describing processes of plastic flow in materials, regardless of their nature and plasticity microscopic mechanisms.

4. AUTOWAVE MODEL OF PLASTIC FLOW

The developed model of nucleation and evolution of localized plastic flow is based on invariant (8), which indirectly indicates the important role of acoustic properties (phonon subsystem) of the crystal in the formation of plastic flow localization autowave patterns. The possible reason is based on the fact that only dislocations moving between the local barriers, for which $V_d \neq 0$, contribute to the macroscopic plastic strain rate $\dot{\epsilon} \approx b\rho_{md}V_{disl}$ [16]. In this case, their motion

Table 2. Comparison of the χV_t and λV_{aw} values for alkali halide crystals and rocks

$10^7 \text{ m}^2/\text{s}$	KCl	NaCl	LiF	Marble	Sandstone
λV_{aw}	3.0	3.1	4.3	1.75	0.6
χV_t	7.0	7.5	8.8	3.7	1.5
$\lambda V_{aw}/\chi V_t$	0.43	0.4	0.5	0.5	0.4

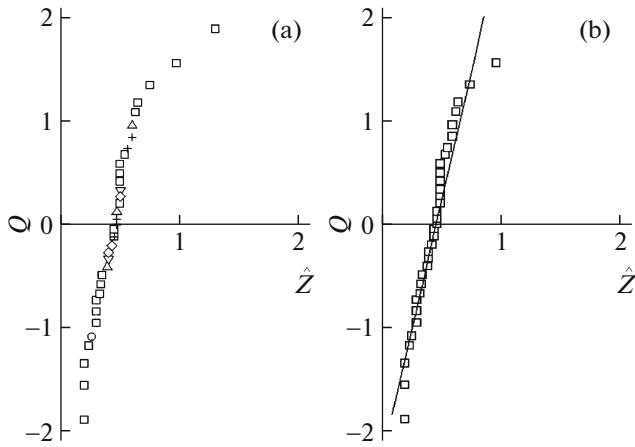


Fig. 3. Dependences $Q(\hat{Z})$ plotted (a) for all data and (b) after excluding the gross error for lead. The correlation coefficient between the Q and \hat{Z} values is ~ 0.98 : (\square) metals (linear strain hardening stage), (\triangle) metals (easy glide stage), (\diamond) alkali halide crystals, (+) mean free paths of dislocations, (∇) rocks, and (\circ) titanium nickelide.

is over-barrier and controlled by the interaction with viscous phonon and electron gases [34]. Their properties determine the plastic flow dynamics, including that at the macroscale (autowave) level.

However, the phonon subsystem in the developed model plays a more important role in the description of the evolution of localized plastic flow of solids. The deformation process including elementary relaxation events is accompanied by two effects occurring in the phonon subsystem of the deformed crystal. The first one is acoustic emission, i.e., generation of elastic waves during relaxation events of deformation. The second one is an acoustoplastic effect consisting in the initiation of plastic shears under ultrasonic pulses applied to the deformed system. Thus, if an elementary relaxation event generates an acoustic pulse, the latter can in turn initiate the development of a new shear in a different crystal region. Both effects have been sufficiently investigated independently of each other; however, the sense of the developed model consists in matching of these mechanisms.

The developed approach is based on the concept of spontaneous stratification of self-organizing systems into information and dynamic subsystems [21]. The choice of these subsystems for the case of strain is

Table 3. Comparison of the χV_t and IV_{disl} values for mean free paths of individual dislocations

$10^7 \text{ m}^2/\text{s}$	NaCl	LiF	CsI	KCl	Zn
IV_{disl}	4.1	4.1	1.9	4.1	1.8
χV_t	7.3	8.6	4.0	6.8	4.0
$IV_{\text{disl}}/\chi V_t$	0.56	0.47	0.47	0.6	0.45

determined by its mechanisms. In an active deformed medium with a set of elastic-stress concentrators, the first subsystem can be related to acoustic emission pulses at shears, while the second one to the shears themselves. Thus, the concentrator elastic field decays at relaxation initiates in turn new shears. The multiple repetitions of these events form a localized plasticity pattern and a corresponding autowave mode. Therefore, the following scenario of plastic flow evolution appears real. Relaxation of the stress concentrator generates an acoustic emission pulse. Its energy absorbed by another concentrator induces a new shear, at which a new acoustic pulse is emitted. Afterwards, these events are repeated.

The plausibility of the model proposed is proven by comparing waiting time τ of a thermally activated event of shear relaxation [35] under only stress σ

$$\tau_1 = f_D^{-1} \exp\left(\frac{U_0 - \gamma\sigma}{k_B T}\right) \approx 5 \times 10^{-5} \text{ s} \quad (18)$$

with similar time under the action of an acoustic pulse with elastic strain amplitude ε_{ac}

$$\tau_2 = f_D^{-1} \exp\left[\frac{U_0 - \gamma(\sigma + \varepsilon_{\text{ac}}E)}{k_B T}\right] \approx 9 \times 10^{-7} \text{ s}. \quad (19)$$

For estimations from formulas (18) and (19), it is assumed that $f_D \approx 10^{13} \text{ Hz}$, activation enthalpy is $U_0 - \gamma\sigma \approx 0.5 \text{ eV}$, $k_B T \approx 0.025 \text{ eV}$, and the application of an acoustic pulse reduces its value by $\gamma\varepsilon_{\text{ac}}E \approx 0.1 \text{ eV}$. Even with allowance for the evident roughness of the calculation, the difference between times τ_1 and $\tau_2 \ll \tau_1$ confirms the validity of the considered mechanism. The estimation of the correlation length for localized strain patterns is also possible; it coincides with the localized plastic flow autowave length. Indeed, $V_t \tau_2 \approx 5 \text{ mm} \approx \lambda$, whereas $v_t \tau_1 \approx 100 \text{ mm} \gg \lambda$, a value comparable to the sample size.

CONCLUSIONS

The point of view on the process of plastic flow, developed in recent years, relates this phenomenon with macroscopic regularities of the strain localization. The performed experiments and interpretation of their results show that this macroscopic consideration of the deformed solid makes it possible to apply an apparatus of the fields of modern science such as synergetics and physics of nonlinear media when discussing the plasticity phenomenon.

As follows from the results reported, the plastic flow is implemented as evolution of autowave processes, which begins at the yield stress and ends at the sample fracture. It is accompanied by a systematic change in macroscopic localization forms (i.e., different autowave modes of localized plastic flow are successively generated, the type of which is determined by the actual strain hardening law.

Based on the developed autowave concepts, we constructed a model of localized plasticity, according to which the evolution of plastic flow is a result of joint action of relaxation dislocation shears and emission—absorption of acoustic emission pulses controlling these shear processes.

Characteristics of the elastic and plastic strains of the deformed medium are related by a simple relation referred to as the elastoplastic strain invariant. The invariant can be considered as the main equation of autowave plasticity mechanics.

FUNDING

This study was performed within the Program of Fundamental Scientific Research of State Academies of Sciences for 2013–2020 (line of research III.23).

CONFLICT OF INTEREST

The authors declare that they do not have a conflicts of interest.

REFERENCES

1. E. Scott, *Nonlinear Science. Emergence and Dynamics of Coherent Structures* (Oxford Univ. Press, Oxford, 2003; Fizmatlit, Moscow, 2007).
2. L. B. Zuev, *Autowave Plasticity. Localization and Collective Mods* (Fizmatlit, Moscow, 2018) [in Russian].
3. L. B. Zuev, S. A. Barannikova, and A. G. Lunev, *From Macro to Micro. The Extent of Plastic Deformation* (Nauka, Novosibirsk, 2018) [in Russian].
4. A. Seeger and W. Frank, in *Non-Linear Phenomena in Materials Science*, Ed. by L. P. Kubin and G. Martin (Trans Tech., New York, 1987), p. 125.
5. H. Haken, *Information and Self-Organization. A Macroscopic Approach to Complex Systems* (Springer, Berlin, Heidelberg, 2006).
6. G. Nicolis and I. Prigogine, *Exploring Complexity: An Introduction* (St. Martin's Press, New York, 1989).
7. U. Messerschmidt, *Dislocation Dynamics during Plastic Deformation* (Springer, Berlin, 2010).
8. W. Walter Grey, *Living Brain* (W. W. Co. Norton, New York, 1963).
9. C. Fressengeas, A. Beaudoin, and D. Entemeyer, *Phys. Rev. B* **79**, 014108 (2009).
<https://doi.org/10.1103/PhysRevB.79.014108>
10. M. A. Lebyodkin, N. P. Kobelev, Y. Bougherira, D. Entemeyer, C. Fressengeas, V. S. Gornakov, T. A. Lebedkina, and I. V. Shashkov, *Acta Mater.* **60**, 3729 (2012).
<https://doi.org/10.1016/j.actamat.2012.03.026>
11. T. V. Tret'yakova and V. E. Vil'deman, *Spatial-Temporal Heterogeneity of the Processes of Inelastic Deformation of Metals* (Fizmatlit, Moscow, 2017) [in Russian].
12. O. A. Plekhov, *Tech. Phys.* **56**, 301 (2011).
<https://doi.org/10.1134/S106378421102023X>
13. L. B. Zuev, *Metallofiz. Noveish. Tekhnol.* **16**, 31 (1994).
14. V. A. Vasil'ev, Yu. M. Romanovskii, and V. G. Yakhno, *Autowave Processes* (Nauka, Moscow, 1987) [in Russian].
15. Yu. B. Rumer and M. Sh. Ryvkin, *Thermodynamics, Statistical Physics and Kinetics* (NGU, Novosibirsk, 2000) [in Russian].
16. A. N. Kolmogorov, I. G. Petrovskii, and N. S. Piskunov, *Byull. Mosk. Univ., Ser. A: Mat. Mekh.* **1**, 6 (1937).
17. A. Cottrell, *Theory of Crystal Dislocations* (Gordon and Breach, London, 1964).
18. J. Pelleg, *Mechanical Properties of Materials* (Springer, Dordrecht, 2013).
19. Sh. Kh. Khannanov and S. P. Nikanorov, *Tech. Phys.* **52**, 70 (2007).
20. T. S. Akhromeeva, S. P. Kurdyumov, G. G. Malinetskii, and A. A. Samarskii, *Structures and Chaos in Nonlinear Media* (Fizmatlit, Moscow, 2007) [in Russian].
21. B. B. Kadomtsev, *Dynamics and Information* (Redakts. UFN, Moscow, 1997) [in Russian].
22. L. B. Zuev, *Bull. Russ. Acad. Sci.: Phys.* **78**, 957 (2014).
<https://doi.org/10.3103/S1062873814100256>
23. Yu. L. Klimontovich, *Introduction to Open Systems Physics* (Yanus-K, Moscow, 2002) [in Russian].
24. L. B. Zuev, S. A. Barannikova, and A. G. Lunev, *Usp. Fiz. Met.* **19**, 379 (2018).
<https://doi.org/10.15407/ufm.19.04.379>
25. L. B. Zuev, *Metallofiz. Noveish. Tekhnol.* **18**, 55 (1996).
26. S. A. Barannikova, M. V. Nadezhkin, and L. B. Zuev, *Tech. Phys. Lett.* **37**, 750 (2011).
<https://doi.org/10.1134/S1063785011080177>
27. L. B. Zuev, S. A. Barannikova, M. V. Nadezhkin, and V. V. Gorbatenko, *Fiz. Tekh. Poluprovodn. RPI*, No. 2, 49 (2014).
28. V. I. Danilov, A. A. Yavorskii, L. B. Zuev, and V. E. Panin, *Russ. Phys. J.* **34**, 283 (1991).
29. L. B. Zuev, V. E. Gromov, V. F. Kurilov, and L. I. Gurevich, *Sov. Phys. Dokl.* **23**, 199 (1978).
30. E. V. Darinskaya and A. A. Urusovskaya, *Sov. Phys. Solid State* **17**, 1601 (1975).
31. E. V. Darinskaya, A. A. Urusovskaya, V. N. Opekunov, G. A. Abramchuk, and V. A. Alekhin, *Sov. Phys. Solid State* **20**, 721 (1978).
32. E. V. Darinskaya, A. A. Urusovskaya, V. I. Al'shits, Yu. I. Meshcheryakov, V. N. Alekhin, and R. Voska, *Sov. Phys. Solid State* **25**, 2092 (1983).
33. M. N. Stepnov, *Probabilistic Methods for Assessing the Characteristics of the Mechanical Properties of Materials* (Nauka, Novosibirsk, 2005) [in Russian].
34. V. I. Al'shits and V. L. Indenbom, in *Dislocations in Solids* (Elsevier, Amsterdam, 1986), p. 43.
35. D. Caillard and J. L. Martin, *Thermally Activated Mechanisms in Crystal Plasticity* (Elsevier, Oxford, 2003).

Translated by A. Sin'kov